Electronic Supplementary Information (ESI)

S.1 Splay energy

Here we show that the elastic splay energy density (Eq. 3)

$$E_{sp} = \frac{1}{2} A_{sp} \kappa^2 \cos^2 \xi \tag{S.1}$$

can be conveniently expressed in terms of the angle between BS and BB bond, χ (see Fig. S.1). As observed from the Figure, $\vec{l} \cdot \vec{b} = \vec{l}_\parallel \cdot \vec{b}$, thus

$$\cos \chi = \cos \xi \cos \frac{\varphi}{2} \tag{S.2}$$

where φ is the angle between two consecutive $\vec{b}$ vectors.
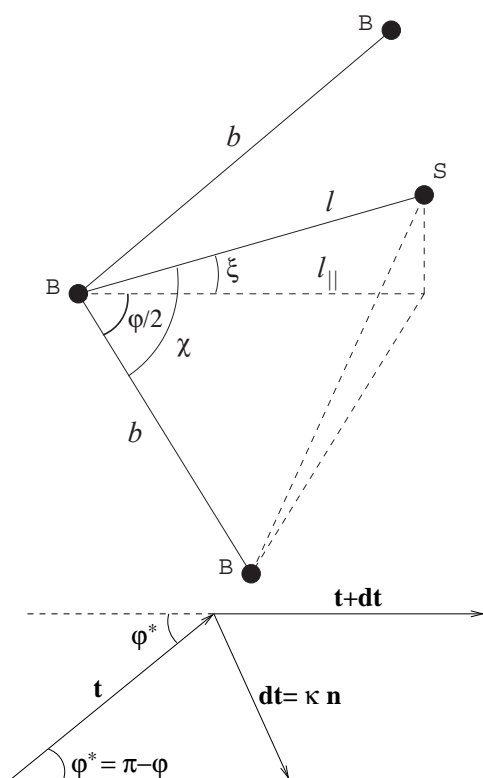

Fig. S.1 Schematic illustrating the relation between the angles ξ, χ and φ

.

Next, let $\mathbf{t}$ and $\mathbf{t} + \mathbf{dt}$ be the two consecutive tangent vectors along the backbone (corresponding, in our case, to the two consecutive *BB* bonds). Then, from the lower panel of Fig. S.1,

$$\tan \varphi^* = \frac{|\mathbf{dt}|}{|\mathbf{t}|} = \kappa, \tag{S.3}$$

where $\varphi* = \pi - \varphi$ has been assumed to be small and the Frenet-Serret equation $\mathbf{dt} = \kappa \mathbf{n}$ has been used. Thus

$$\cos^2 \frac{\varphi}{2} = \frac{1}{2}\left(1 - \frac{1}{\sqrt{1 + \kappa^2}}\right) \overset{\kappa \ll 1}{\approx} \frac{\kappa^2}{4} \tag{S.4}$$

and the splay energy can be written as

$$E_{sp} = 2 A_{sp} \cos^2 \chi \tag{S.5}$$

S.2 Curvature, pitches, and radii of the helices

The curvature of an ideal helix with helical angle α and radius R is $\kappa = \frac{\sin^2 \alpha}{R}$. Hence, using eq. S.3, the radius is:

$$R = \frac{\sin^2 \alpha}{\tan \varphi^*} \tag{S.6}$$

and pitch of the helix ($P = 2\pi R \cot \alpha$):

$$P = \frac{2\pi \cos \alpha}{\tan \varphi^*}. \tag{S.7}$$

Both, α and φ^* can be retrieved from the simulation data. The distributions of pitch values obtained from eq. S.7 is presented in Fig. S.2. As observed, the average pitch is almost independent of the value of the internal twist of the individual filaments, λ_0. It oscillates between $23.15°$ and $23.45°$. Hence, it was assumed to be constant in the simplified theoretical model presented in the main text.
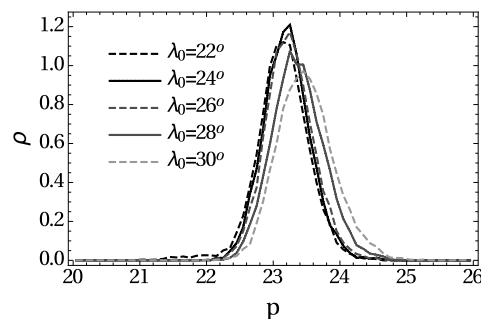

Fig. S.2 Distribution of pitch values of the tubular structures obtained in the simulations for several λ_0 values.

S.3 Force field parameters

The force field in the model is constructed analogously to that in Ref. 34. The total bond energy is the sum of four contributions:

$$U_{bond} = U_{lBB} + U_{lBS} + U_\varphi + U_\chi + U_\theta + U_\lambda, \tag{S.8}$$

with:

$$U_{lBB} = \frac{k_{lBB}}{2}(l^{BB} - l_0^{BB})^2$$

$$U_{lBS} = \frac{k_{lBS}}{2}(l^{BS} - l_0^{BS})^2$$

$$U_{\varphi} = \frac{k_{\varphi}}{2}(\varphi - \varphi_0)^2$$

$$U_{\chi} = \frac{k_{\chi}}{2}(\chi - \chi_0)^2$$

$$U_{\theta} = 1 + a_2\theta^2 + \theta^4 + a_6\theta^6$$

$$U_{\lambda} = \frac{k_{\lambda}}{2}(\lambda - \lambda_0)^2 \qquad \text{(S.9)}$$

where l^{BB} and l^{BS} are the distances between the neighboring backbone beads and between the B bead and the adjacent S bead respectively. Next, the bond angles φ and χ are the angles between three successive B beads (BBB) and between S bead and two B beads (as marked in Fig. S.1). Dihedral angles (see Fig. 1 in the main text) are denoted by λ and θ. The parameters of the force field are given in Table S.1. The values of a_2 and a_6 were computed for each θ_0 to get the potential with minima at $\pm\theta_0$ and a barrier height of $\Delta E = 5/2$.

term	beads affected	parameters
U_{lBB}	$B - B$	$k_{lBB} = 100, l_0^{BB} = 1$
U_{lBS}	$B - S$	$k_{lBS} = 50, l_0^{BS} = 2$
U_{φ}	$S - B - B$	$k_{\varphi} = 200, \varphi_0 = \pi/2$
U_{χ}	$B - B - B$	$k_{\chi} = 50, \chi_0 = \pi$
U_{λ}	$S - B_i B_{i+2} - S$	$k_{\lambda} = 10$
U_{θ}	$S1 - B_i B_{i+1} - S2$	a_2 and a_6 - see the text
LJ	B	$\varepsilon = 1, \sigma_B = 4$
LJ	$S1, S2$	$\varepsilon = 1, \sigma_S = 1$

Table S.1 Force field parameters

The energy contributions presented in Figs. 12 and 14 in the main text are the mean values of the above terms over the entire 3-filament cluster, e.g.

$$u_{lBB} = \frac{1}{n}\sum_{BB\ bonds} U_{lBB}$$

$$u_{\varphi} = \frac{1}{n}\sum_{\varphi} U_{\varphi}$$

and analogously for other components. Here the sums are taken over all bonds, angles, dihedrals or bead pairs in the 3-filament cluster. The sum is then divided by $n = 180$, which is the number of elementary units in the system (3 chains 60 B beads each) to get the energy per unit length of the chain. The individual contributions to the internal energy of different structural forms, additionally averaged over the simulation trajectory, are presented in Fig. S.3 below.

S.4 Binding energies for different structural forms

As mentioned in the main text, the cohesive interactions between the filaments are relatively strong (compared to the energy of elastic deformations), which leads us to assume that the energy of each contact between the beads is simply $-\varepsilon$ (corresponding to the depth of the energy well). There are approximately 450 contacts in 3-filament clusters of a tubular and helicoidal form (180 B-B contacts, 90 S-S contacts and 180 S-B contacts), which gives on the average 2.5 contacts per unit length of each filament. An analogous calculation for the ribbons gives the value of 1.67 contacts per unit length. In fact it is a rough estimate only, since it neglects the interactions between the beads from different layers. Summing up:

$$E_{int}/L; = \begin{cases} -2.5\varepsilon & \text{helicoid, tubule} \\ -1.67\varepsilon & \text{ribbon} \end{cases} \qquad \text{(S.10)}$$

S.5 Bending energies and splay

In Eq. 3 in the main text, the elastic energy has been put in the form

$$E_{el} = \frac{1}{2}\int_0^L \left(A_1\kappa^2(s) + A_{sp}\kappa^2(s)\cos^2(\xi) + C(\tau(s) - \hat{\tau}_0)^2\right)ds. \qquad \text{(S.11)}$$

with the first term standing for the isotropic bending, whereas the second (splay) gives the extra energy which is associated with bending along one axis in comparison to the other. The above terms are easily related to the energy contributions in the numerical model: the isotropic part will be the one associated with bending of the backbone (i.e. φ angles) whereas the anisotropic part is connected with the presence of the side strand (i.e. χ angles). Thus:

$$A_1 = k_{\varphi} \qquad A_{sp} = \frac{1}{4}k_{\chi} \qquad \text{(S.12)}$$

(see Sec. S.1 for the origin of the factor of 4).

S.6 Twist rigidity constant

Twist elasticity enters the system Hamiltonian through the two dihedral angles, θ and λ (see Eq. S.9 and Fig. 1 in the main text). However, in different structures these angles are constrained in a different way:

- For helicoidal structures in binding mode $n = 1$ (Fig. 5a) the interaction seam is maintained by every other backbone bead, with their relative location controlled by λ, whereas θ angles are effectively unconstrained. In this case the angular elasticity is controlled by the U_{λ} term in the Hamiltonian, hence $C = k_{\lambda}$ is assumed.

- For helicoidal structures in binding mode $n = 5$ (Fig. 5b) both side-strands participate in the interaction seam, which constraints the values of both θ and λ angles. However, the curvature of the U_θ potential at the minimum, $k_\theta = 2U_\theta''(\theta_0)$ is much larger than k_λ, thus $C \approx k_\theta$ can be assumed here

- In the twisted ribbon structures (Fig. 2c) each side strand interact with its counterpart on the other filament, which again constraints λ, thus $C = k_\lambda$ can be taken here. The elastic energy of these structures is simply $k_\lambda \hat{\tau}_0^2$.

- Tubular structures (Fig. 2d) are maintained by the contact involving both side-strands, hence $C = k_\theta$ is assumed here.

S.7 Videos

Two videos are available as a supplementary material to the present article:

- helicoid_to_tubule.mpg - a video illustrating the helicoid to tubule transition

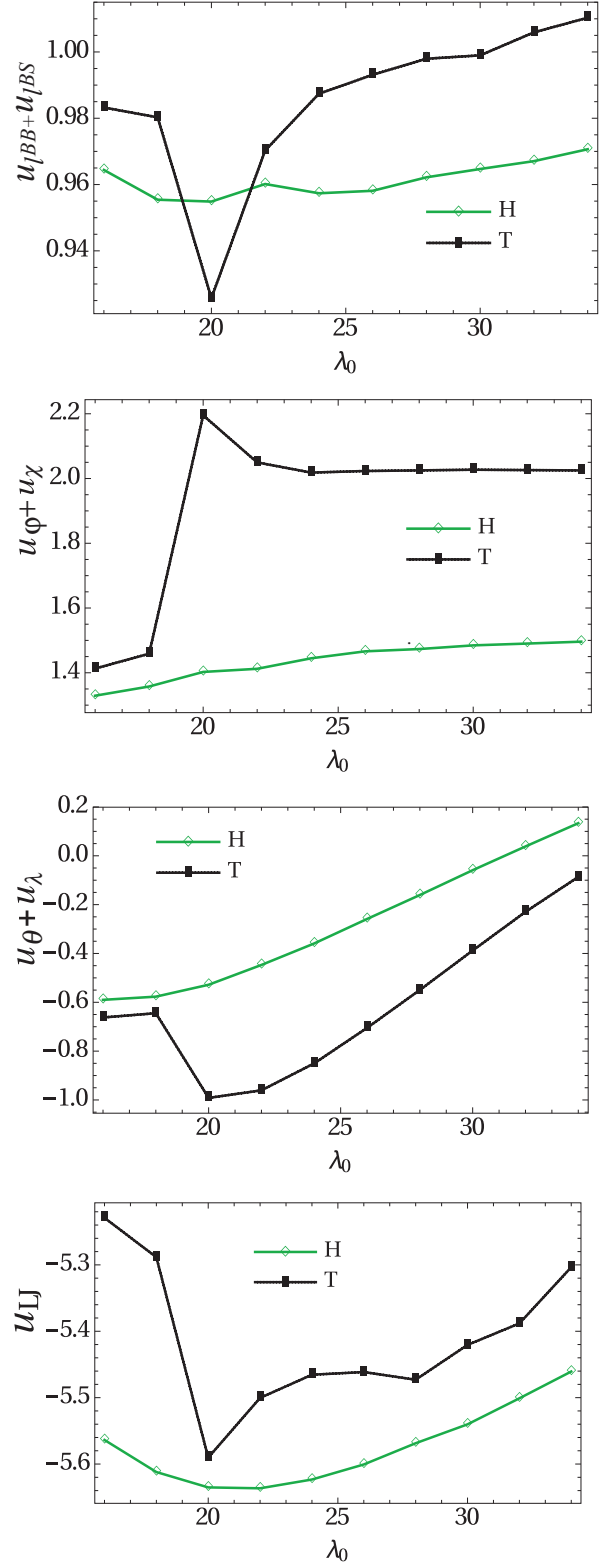- tubule_to_helicoid.mpg - a video illustrating the tubule to helicoid transition

Fig. S.3 Bond, angle, dihedral and LJ energies per monomer in the tubule (black) and helicoidal (green) systems for different values of internal twist of the filaments, λ_0.